ALIEN EARTHS

Which Nearby Planetary Systems Are Likely to Host Habitable Planets and Life?

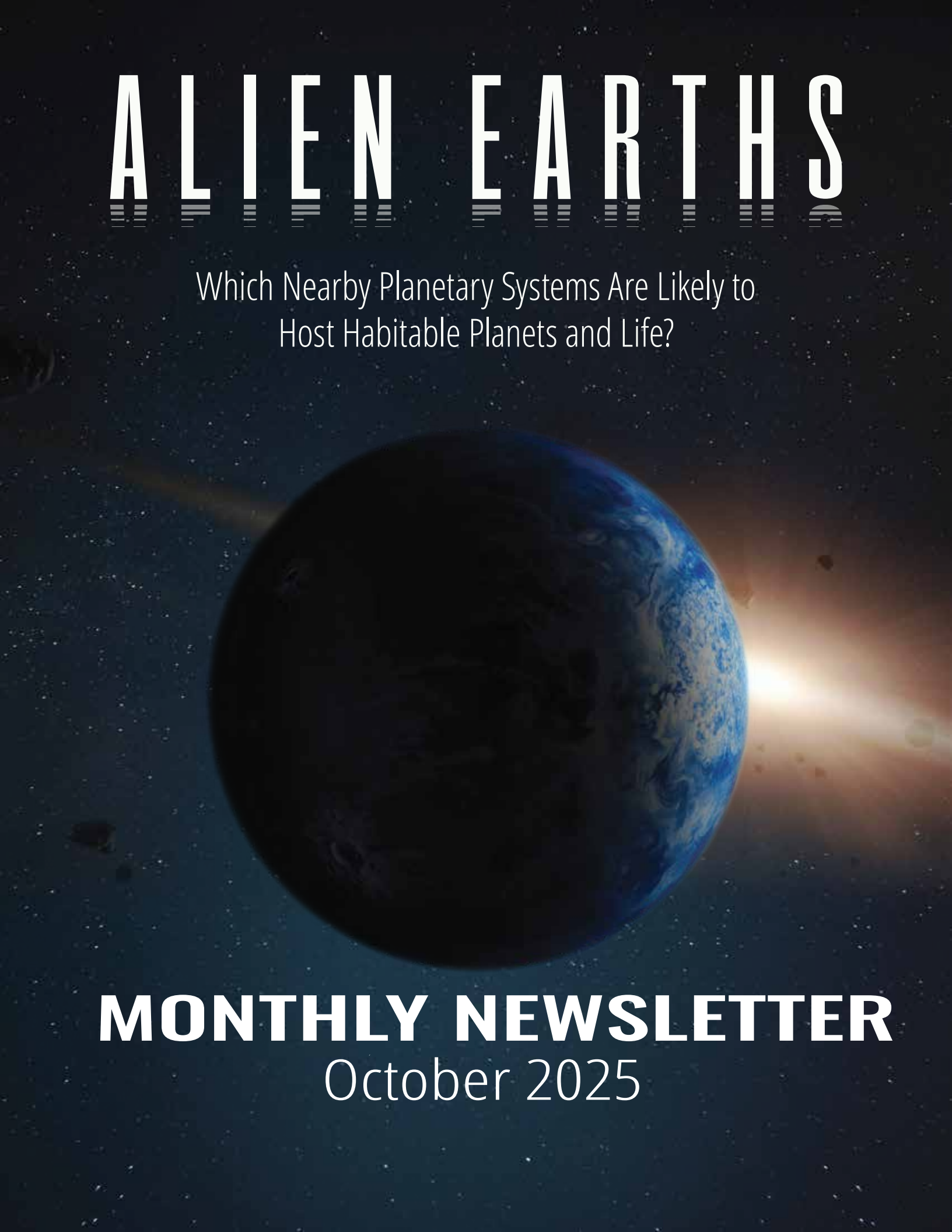

MONTHLY NEWSLETTER

October 2025

Alien Earths is part of NASA's Nexus for Exoplanetary System Science program, which carries out coordinated research toward the goal of searching for and determining the frequency of habitable extrasolar planets with atmospheric biosignatures in the Solar neighborhood.

Our interdisciplinary teams includes astrophysicists, planetary scientists, cosmochemists, material scientists, chemists, biologists, and physicists.

The Principal Investigator of Alien Earths is Daniel Apai (University of Arizona). The projects' lead institutions are The University of Arizona's Steward Observatory and Lunar and Planetary Laboratory.

For a complete list of publications, please visit the AE Library on the SAO/NASA Astrophysics Data System.

Recent Publications

Cosmic Cascades: How Disk Substructure Regulates the Flow of Water to Inner Planetary Systems

Wide Separation Planets in Time (WISPIT): Discovery of a Gap Hα Protoplanet WISPIT 2b with MagAO-X

The vertical structure of debris discs and the role of disc gravity: A primer using a simplified model

DiskMINT: Self-Consistent Thermochemical Disk Models with Radially Varying Gas and Dust -- Application to the Massive, CO-Rich Disk of IM Lup

Astrometric Methods for Detecting Exomoons Orbiting Imaged Exoplanets: Prospects for Detecting Moons Orbiting a Giant Planet in α Centauri A's Habitable Zone

Lunar impact ejecta flux on the Earth

From Colors to Spectra and Back Again: First Near-IR Spectroscopic Survey of Neptunian Trojans

Runaway origins of a disc mass gradient in σ Orionis

Bioverse: Assessing the Ability of Direct Imaging Surveys to Empirically Constrain the Habitable Zone via Trends in Albedo

Save the Date!

Mark your calendars, the 2026 Alien Earths All Hands Meeting will take place February 3 - February 6 in Tucson.

Cosmic Cascades: How Disk Substructure Regulates the Flow of Water to Inner Planetary Systems

Krijt, Sebastiaan; Banzatti, Andrea; Zhang, Ke; Pinilla, Paola; Kaeufer, Till; Bergin, Edwin A.; Salyk, Colette; Pontoppidan, Klaus; Blake, Geoffrey A.; Long, Feng; Huang, Jane; Colmenares, María José; Williams, Joe; Houge, Adrien; Narang, Mayank; Vioque, Miguel; Lambrechts, Michiel; Cleeves, L. Ilsedore; Öberg, Karin; The Jdiscs Collaboration

The Astrophysical Journal Letters, Volume 990, Issue 2, id.L72, 12 pp.

The influx of icy pebbles to the inner regions of protoplanetary disks constitutes a fundamental ingredient in most planet formation theories. The observational determination of the magnitude of this pebble flux and its dependence on disk substructure (disk gaps as pebble traps) would be a significant step forward. In this work, we analyze a sample of 21 T Tauri disks (with ages ≈0.5–2 Myr) using JWST/MIRI spectra homogeneously reduced with the JDISCS pipeline and high-angular-resolution Atacama Large Millimeter/submillimeter Array (ALMA) continuum data. We find that the 1500/6000 K water line flux ratio measured with JWST—a tracer of cold water vapor and pebble drift near the snow line—correlates with the radial location of the innermost dust gap in ALMA continuum observations (ranging from 8.7 to 69 au), confirming predictions from recent models that study connections between the inner and outer disk reservoirs. We develop a population synthesis exploration of pebble drift in gapped disks and find a good match to the observed trend for early and relatively effective gaps, while scenarios where pebble drift happens quickly, gaps are very leaky, or where gaps form late, are all disfavored on a population level. Inferred snow line pebble mass fluxes (ranging between 10-6 and 10-3 M⊕ yr-1 depending on gap position) are comparable to fluxes used in pebble accretion studies and those proposed for the inner solar system, while system-to-system variations suggest differences in the emerging planetary system architectures and water budgets.

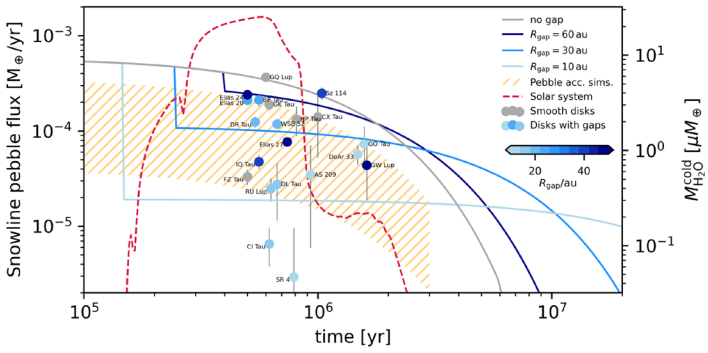

***Figure 2**. Compilation of pebble mass flux vs. time evolutions. Solid lines show models developed in this study for various gap positions (see Section 3.1), which can be compared to mass fluxes required in pebble accretion simulations to form diverse inner planetary systems (dashed area; see M. Lambrechts et al. 2019) and the pebble mass flux inferred for the inner solar system using models capable of matching the non-carbonaceous (NC) and carbonaceous (CC) chondrite isotopic dichotomy (red dashed; see T. Lichtenberg et al. 2021). Symbols show ages and cold water masses of all 21 objects in our sample computed from JWST/MIRI line ratios (Table 1) in combination with Equation (4) (see Appendix A), and the left and right y-axes are related through Equation (3). Symbol color corresponds to inner gap position as obtained from high-spatial-resolution ALMA observations (see Section 2), and error bars reflect uncertainties in measured line ratios.*

Wide Separation Planets in Time (WISPIT): Discovery of a Gap Hα Protoplanet WISPIT 2b with MagAO-X

Close, Laird M.; van Capelleveen, Richelle F.; Weible, Gabriel; Wagner, Kevin; Haffert, Sebastiaan Y.; Males, Jared R.; Ilyin, Ilya ; Kenworthy, Matthew A.; Li, Jialin; Long, Joseph D.; Ertel, Steve ; Ginski, Christian; Weinberger, Alycia J.; Follette, Kate; Liberman, Joshua; Twitchell, Katie; Johnson, Parker ; Kueny, Jay; Apai, Daniel; Doyon, Rene; Foster, Warren ; Gasho, Victor ; Van Gorkom, Kyle; Guyon, Olivier; Kautz, Maggie Y.; McLeod, Avalon ; McEwen, Eden; Pearce, Logan ; Schatz, Lauren ; Hedglen, Alexander D. ; Wu, Ya-Lin; Isbell, Jacob; Power, Jenny ; Carlson, Jared ; Close, Emmeline; Tonucci, Elena; Mars, Matthijs

The Astrophysical Journal Letters, Volume 990, Issue 1, id.L9, 15 pp.

Excellent (<25 mas) Hα images of the star TYC 5709-354-1 led to the discovery of a rare Hα protoplanet. This star was discovered by the WISPIT survey to have a large multi-ring transitional disk, and is hereafter WISPIT 2. Our Hα images of 2025 April 13 and 16 discovered an accreting (H α in emission) protoplanet: WISPIT 2b (r = 309.43 $\pm$ 1.56 mas; (~54 au deprojected), PA = 242 .$^{\circ}$ 21 $\pm$ 0 .$^{\circ}$ 41) likely clearing a dust-free gap between the two brightest dust rings in the transitional disk. Our signal-to-noise ratio of 12.5 detection gave an Hα ASDI contrast of (6.5 ± 0.5) × 10-4 and an Hα line flux of (1.29 ± 0.28) × 10-15 erg s-1 cm-2. We also present L' photometry from LBT/LMIRcam of the planet (L' = 15.30 ± 0.05 mag), which, when coupled with an age of 5.1-1.3+2.4 Myr, yields a planet mass estimate of 5.3 ± 1.0 Mjup from the DUSTY evolutionary models. WISPIT 2b is accreting at 2.25-0.17+3.75 × 10-12 MSun yr-1. WISPIT 2b is very similar to the other Hα protoplanets in terms of mass, age, flux, and accretion rate. The inclination of the system (i = 44°) is also, surprisingly, very similar to the other known H α protoplanet systems, which all cluster from 37° $\leq$ i $\leq$ 52° . We argue this clustering has only a ~1.0% (2.6 σ) probability of occurring randomly, and so we speculate that magnetospherical accretion might have a preferred inclination range (~37° −52°) for the direct (cloud free, low extinction) line of sight to the H α line formation/shock region. We also find at 110 mas (~15 au deprojected) a close companion candidate (CC1) that may be consistent with an inner dusty 9 ± 4 Mjup planet.

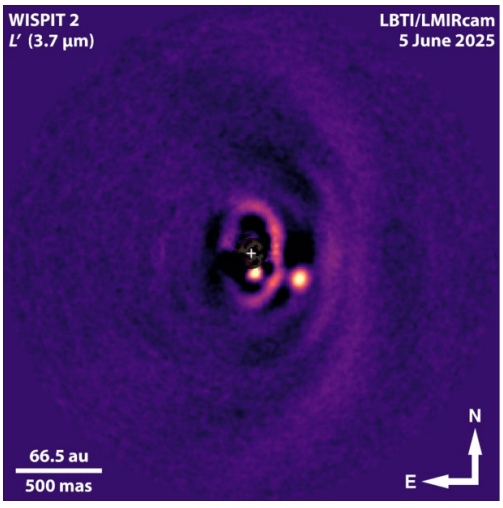

Figure 2. *The KLIP reduced L′ image from the LBT telescope with the LBTI LMIRcam instrument. The location of WISPIT 2b and the inner #3 and outer #2 dust rings are clear (despite the significant self-subtraction from KLIP). WISPIT 2b is located nearly in the center of the dust-free gap between the rings. The image is 1.''43 × 1.''43; see Appendix B for details about the L′ reduction.*

The vertical structure of debris discs and the role of disc gravity: A primer using a simplified model

Antranik A Sefilian, Kaitlin M Kratter, Mark C Wyatt, Cristobal Petrovich, Philippe Thébault, Renu Malhotra, Virginie Faramaz-Gorka

Monthly Notices of the Royal Astronomical Society, 2025;, staf1555

Debris discs provide valuable insights into the formation and evolution of exoplanetary systems. Their structures are commonly attributed to planetary perturbations, serving as probes of as-yet-undetected planets. However, most studies of planet-debris disc interactions ignore the disc's gravity, treating it as a collection of massless planetesimals. We develop a simplified analytical modelasaprimertoinvestigate how the vertical structure of a back-reacting debris disc responds to secular perturbations from an inner, inclined planet. Considering the disc's axisymmetric potential, we identify two dynamical regimes: planet-dominated and disc-dominated, which maycoexist, separated by a secular-inclination resonance. In the planet-dominated regime ($Md/mp \ll 1$), werecover the classical result: a transient warp propagates outward until the disc settles into a box-like structure centered around the planetary orbit's initial inclination $Ip(0)$, with a distance-independent aspect ratio H(R) $\approx Ip(0)$. In contrast, in the disc-dominated regime ($Md/mp \gtrsim 1$), the disc exhibits dynamical rigidity, remaining thin and misaligned, with significantly suppressed inclinations and a sharply declining aspect ratio, H(R) $\propto Ip(0)R-7/2$. In the intermediate regime ($Md/mp \lesssim 1$), the system exhibits a secular-inclination resonance, leading to long-lived, warp-like structures and a bimodal inclination distribution, containing both dynamically hot and cold populations. We provide analytic formulae describing these effects as a function of system parameters. We also find that the vertical density profile is intrinsically non-Gaussian and recommend fitting observations with non-zero slopes of H(R). Our results may be used to infer planetary parameters and debris disc masses based on observed warps and scale heights, as demonstrated for HD 110058 and β Pic.

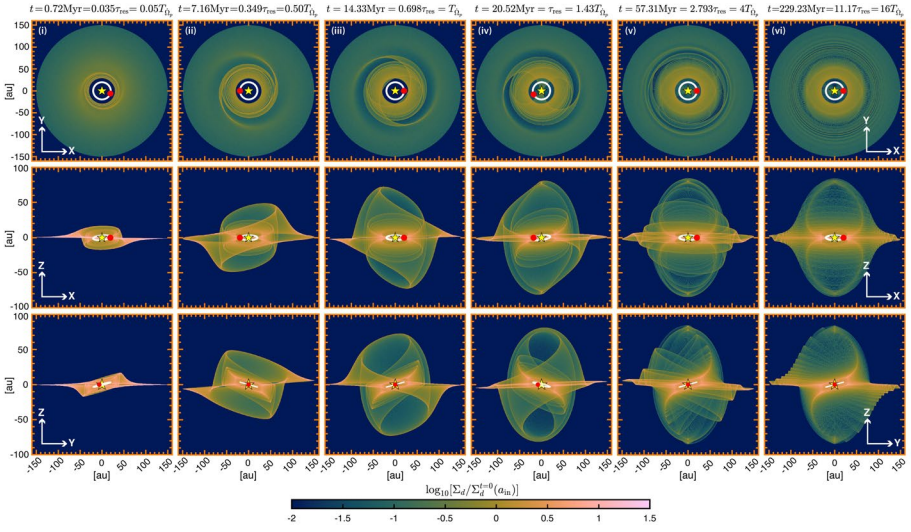

Figure 9*. Snapshots showing the time evolution of the surface density of a debris disk of ≈ 30 Earth masses interacting with an inner inclined planet of 1 Jupiter mass. Different columns correspond to different times (as indicated), and rows show three viewing orientations: face-on (top), end-on (middle), and edge-on (bottom).*

DiskMINT: Self-Consistent Thermochemical Disk Models with Radially Varying Gas and Dust -- Application to the Massive, CO-Rich Disk of IM Lup

Deng, Dingshan search by orcid ; Gorti, Uma ; Pascucci, Ilaria ; Ruaud, Maxime

eprint arXiv:2509.15487

Disks around young stars are the birthplaces of planets, and the spatial distribution of their gas and dust masses is critical for understanding where and what types of planets can form. We present self-consistent thermochemical disk models built with DiskMINT, which extends its initial framework to allow for spatially decoupled gas and dust distributions. DiskMINT calculates the gas temperature based on thermal equilibrium with dust grains, solves vertical gas hydrostatic equilibrium, and includes key processes for the CO chemistry, specifically selective photodissociation, and freeze-out with conversion of CO/CO2 ice. We apply DiskMINT to study the IM Lup disk, a large, massive disk, yet with an inferred CO depletion of up to 100 based on earlier thermochemical models. By fitting the multi-wavelength SED along with the millimeter continuum, C18O radial emission profiles, we find 0.02−0.08 M⊙ for the gas disk mass, which is consistent with the dynamical-based mass within the uncertainties. We further compare the derived surface densities for dust and gas and find that the outer disk is drift-dominated, with a dust-to-gas mass ratio of approximately 0.01-0.02, which is likely insufficient to meet the conditions for the streaming instability to occur. Our results suggest that when interpreted with self-consistent thermochemical models, C18O alone can serve as a reliable tracer of both the total gas mass and its radial distribution. This approach enables gas mass estimates in lower-mass disks, where dynamical constraints are not available, and in fainter systems where rare species like N2H+ are too weak to detect.

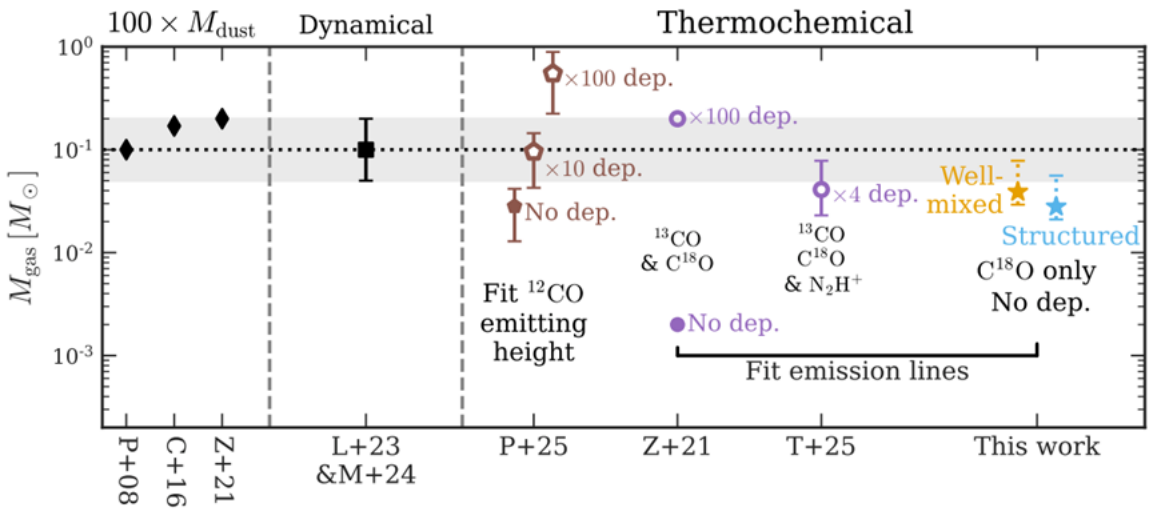

***Figure 9**. Mgas estimates in the literature. Mgas estimates in the literature. From left to right, they include Mgas based on Mdust multiplied by a constant ISM gas-to-dust mass ratio of 100 from P+08 (C. Pinte et al. 2008), C+16 (L. I. Cleeves et al. 2016), Z+21 (K. Zhang et al. 2021), the dynamical Mgas by L+23 & M+24 (G. Lodato et al. 2023; P. Martire et al. 2024), the Mgas inferred from the 12CO emitting height by P+25 (T. Paneque-Carre˜no et al. 2025), and the Mgas inferred from the CO isotopologue line fluxes by Z+21(K. Zhang et al. 2021), T+25 (L. Trapman et al. 2025a), and this work.*

Lunar impact ejecta flux on the Earth

Castro-Cisneros, Jose Daniel; Malhotra, Renu; Rosengren, Aaron J.

Icarus, Volume 438, id.116606

The transfer of material between planetary bodies due to impact events is important for understanding planetary evolution, meteoroid impact fluxes, the formation of near-Earth objects (NEOs), and even the provenance of volatile and organic materials at Earth. This study investigates the dynamics and fate of lunar ejecta reaching Earth. We employ the high-accuracy IAS15 integrator within the REBOUND package to track for 100,000 years the trajectories of 6,000 test particles launched from various lunar latitudes and longitudes. Our model incorporates a realistic velocity distribution for ejecta fragments (tens of meters in size), derived from large lunar cratering events. Our results show that 22.6% of lunar ejecta collide with Earth, following a power-law $C(t) \propto t^{0.315}$, with half of the impacts occurring within ~10,000 years. We also confirm that impact events on the Moon's trailing hemisphere serve as a dominant source of Earth-bound ejecta, consistent with previous studies. Additionally, a small fraction of ejecta remains transiently in near-Earth space, providing evidence that lunar ejecta may contribute to the NEO population. This aligns with recent discoveries of Earth co-orbitals such as Kamoóalewa (469219, 2016 HO3) and 2024 PT5, both exhibiting spectral properties consistent with lunar material. These findings enhance our understanding of the lunar ejecta flux to Earth, providing insights into the spatial and temporal patterns of this flux and its broader influence on the near-Earth environment.

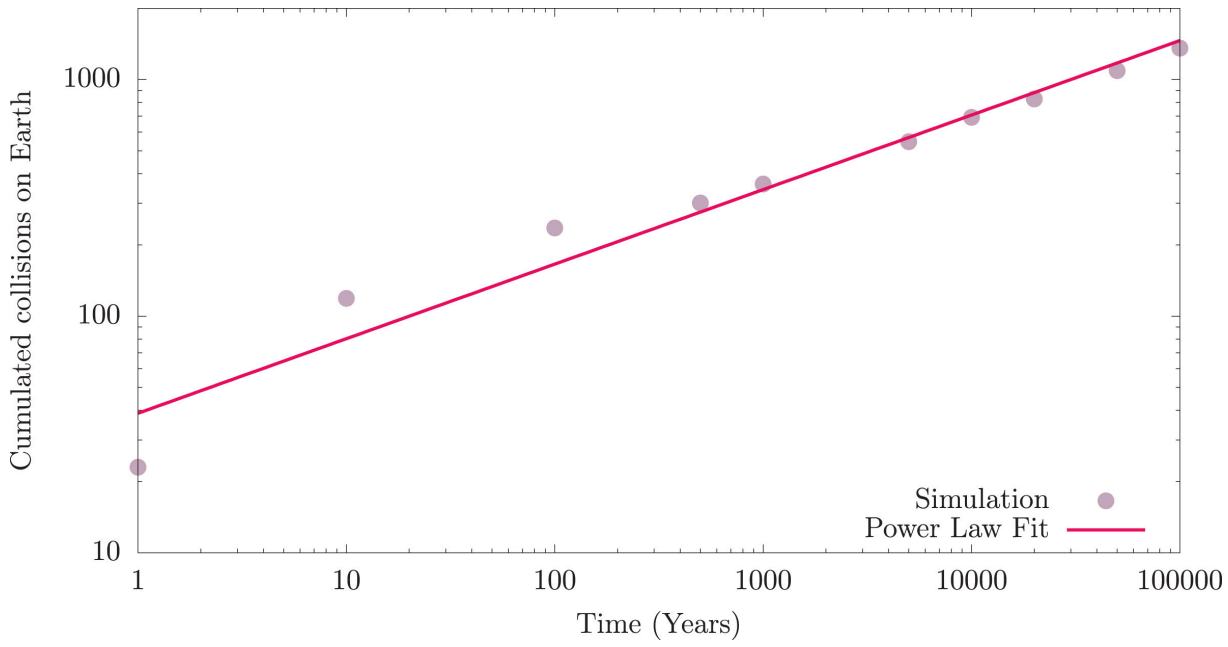

***Figure 4**. Cumulative number of lunar ejecta collisions with Earth over time, on a log–log scale. This scale shows that the late behavior is consistent with a power-law (see Eq. (1)).*

From Colors to Spectra and Back Again: First Near-IR Spectroscopic Survey of Neptunian Trojans

Markwardt, Larissa; Wen Lin, Hsing; Holler, Bryan J.; Gerdes, David W.; Adams, Fred C.; Malhotra, Renu; Napier, Kevin J.

The Planetary Science Journal, Volume 6, Issue 7, id.154, 13 pp.

In this work, we present 0.7–5.0 μm spectra of eight Neptunian Trojans (NTs) as observed by the JWST's NIRSpec instrument. The reddest NT, 2013 VX30, exhibits a unique spectrum with strong absorption features between 3 and 4 μm, while the bluest NT, 2006 RJ103, shows negligible water absorption. A principal component analysis comparing these spectra with those of trans-Neptunian objects (TNOs) and Centaurs reveals that most NTs belong to the "bowl-type" spectral group, while 2013 VX30 is categorized as "cliff-type" in the N. Pinilla-Alonso et al. taxonomy. For the bluest NT in our sample, 2006 RJ103 shows some evidence that it may be related to carbonaceous asteroids. For the red object 2011 SO277, we find no close TNO spectral counterpart. Except for the true outlier 2011 SO277, NTs have better spectral analogs among Plutinos and distant Centaurs, suggesting that spectral variation within major groups may arise from current temperature and location, rather than solely from formation regions. Finally, we highlight optical slope (S') and near-IR slope (SIR1) as effective indicators for distinguishing spectral groups and identifying outliers. These findings enable the use of broadband photometry to explore NT and TNO surface compositions, especially for faint objects, which will be directly applicable to large photometric surveys like the Dark Energy Survey and the Vera C. Rubin Observatory's LSST.

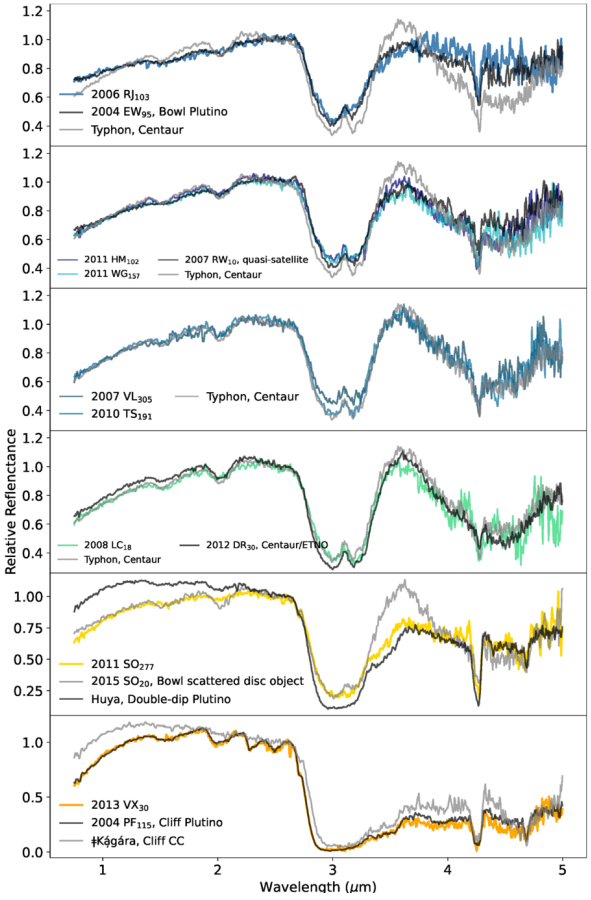

Figure 3. *The spectra of NTs (colored) and their counterparts (gray and black), based on minimizing the sum of the squares of the residuals between the NT and TNO spectra.*

Runaway origins of a disc mass gradient in σ Orionis

Coleman, Gavin A. L. ; Haworth, Thomas J. ; Kim, Jinyoung Serena

eprint arXiv:2509.20227

Radiation from massive stars is known to significantly affect the evolution of protoplanetary discs around surrounding stars by driving external photoevaporative winds. Typically most studies assume that the massive stars driving these winds are comoving with their associated clusters. However, it is also known that massive stars can be runaways, after being violently ejected from their birth environment through interactions with other massive stars. In this letter, we show that the well studied system $σ~{\rm Ori~AB}$ is actually a runaway system, only now passing through $σ~{\rm Orionis}$. There are multiple observable features that indicate this is the case, including significantly larger proper motions for $σ~{\rm Orionis}$ than the surrounding stars, an infrared arc of ionising gas along the predicted velocity vector, and a disparity in protoplanetary disc masses across $σ~{\rm Orionis}$. We finally use protoplanetary disc evolution models to explain the observed disparity in disc masses, showing that those discs downstream of $σ~{\rm Ori~AB}$, i.e. those yet to encounter it, have larger masses than those upstream, consistent with observations. Overall, our work highlights the importance of understanding the dynamical history of star forming regions, since the time varying UV fields provided by runway stars results in a complex history for the evolution of the protoplanetary discs.

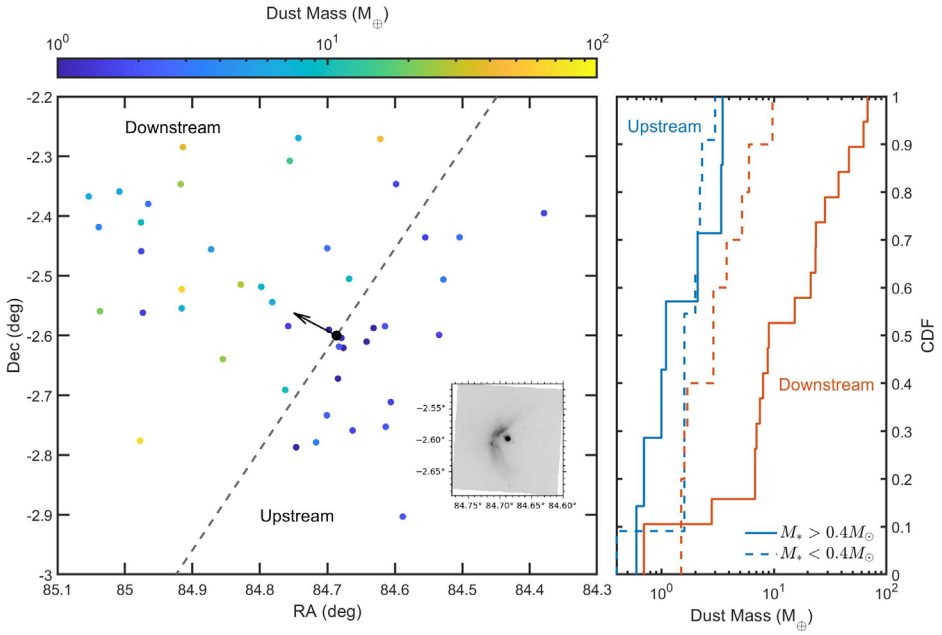

***Figure 1**. Left-hand panel: A 2D map of σ Orionis, with the colour showing the observed disc mass (Mauc´o et al. 2023). The black dot represents σ Ori AB with the arrow showing its ˙proper motion and expected movement over the next 10,000 years. The grey dashed line represents the normal to the trajectory of σ Ori AB, splitting the region into a "downstream" and an "upstream". The inset plot shows a Spitzer image of the infrared arc. (Rieke et al. 2004) Right-hand panel: Cumulative distribution functions for the observed dust disc masses in σ Orionis, split into an upstream region (blue lines) and a downstream region (red lines). Solid lines show the masses for stars more massive than 0.4M⊙, with dashed lines showing for those less massive than 0.4M⊙.*

Bioverse: Assessing the Ability of Direct Imaging Surveys to Empirically Constrain the Habitable Zone via Trends in Albedo

Tuchow, Noah W. ; Stark, Christopher C. ; Apai, Daniel ; Schlecker, Martin ; Hardegree-Ullman, Kevin K.

eprint arXiv:2509.07297

Will future direct imaging missions such as NASA's upcoming Habitable Worlds Observatory (HWO) be able to understand Earth-sized planets as a population? In this study, we simulate the ability of space-based coronagraphy missions to uncover trends in planetary albedo as a function of instellation, and potentially constrain the boundaries of the habitable zone. We adapt the Bioverse statistical comparative planetology framework to simulate the scientific output of possible designs for HWO. With this tool, we generate a synthetic planetary population with injected population-level trends in albedo and simulate the observability of planets. We then determine the statistical power to which these trends can be recovered as a function of the strength of the injected trend and the sample size of Earth-sized planets in the habitable zone (exoEarths). The strongest trends in albedo require a sample size of roughly 25-30 exoEarths to recover with high confidence. However, for weaker albedo trends, the required number of planets increases rapidly. If a mission is designed to meet the Decadal Survey's requirement of 25 exoEarths, it would be able to recover very strong trends in albedo associated with the habitable zone, but would struggle to confidently detect weaker trends. We explore multiple strategies to increase one's ability to recover weak trends, such as reducing the uncertainties in observables, incorporating additional observables such as planet colors, and obtaining direct constraints on planetary albedo from full spectral retrievals.

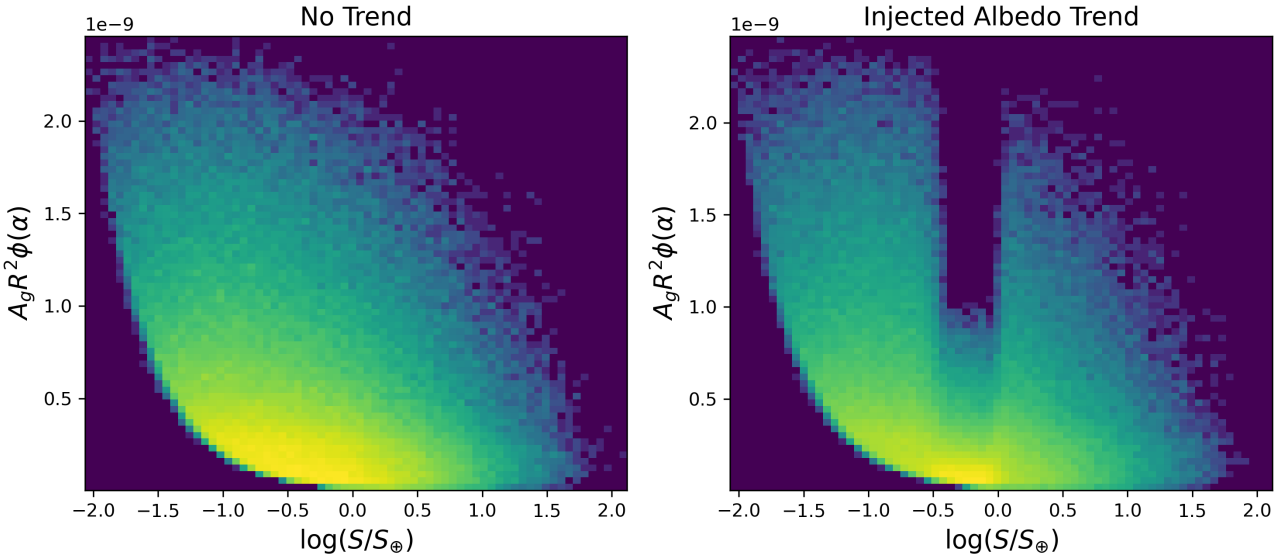

***Figure 2**. Survey distribution of rocky planets that would be detectable for a space-based direct imaging survey with an 8m diameter telescope. Left panel shows the distribution of planets if there is no injected trend in albedo, while the right panel shows the case where there is a strong trend in albedo (ΔA = 0.4). This distribution was generated by simulating the output of exoEarth surveys (analogous to Figure 1) for 1000 simulated universes. Plots are color-coded based on the number of recovered planets in each bin. One can clearly see the influence of population-level trends in albedo in the output, where there is a prominent dip at instellations corresponding to the HZ.*